Available online at www.sciencedirect.com
ScienceDirect
Journal of Power Sources 160 (2006) 782–788
JOURNAL OF POWER SOURCES
www.elsevier.com/locate/jpowsour

Corrosion of anode current collectors in molten carbonate fuel cells

Sara Randström [a,*], Carina Lagergren [a], Paolo Capobianco [b]

[a] KTH Chemical Science and Engineering, Department of Chemical Engineering and Technology, SE-100 44 Stockholm, Sweden
[b] Ansaldo Fuel Cells S.p.A, Corso Perrone 25, I-161 61 Genova, Italy

Available online 6 June 2006

Abstract

Corrosion of metallic parts is one of the life-time limiting factors in the molten carbonate fuel cell. In the reducing environment at the anode side of the cell, the corrosion agent is water. As anode current collector, a widely used material is nickel clad on stainless steel since nickel is stable in anode environment, but a cheaper material is desired to reduce the cost of the fuel cell stack. When using the material as current collector one important factor is a low resistance of the oxide layer formed between the electrode and the current collector in order not to decrease the cell efficiency. In this study, some candidates for anode current collectors have been tested in single cell molten carbonate fuel cells and the resistance of the oxide layer has been measured. Afterwards, the current collector was analysed in scanning electron microscope (SEM) equipped with energy dispersive spectrometer (EDS). The results show that the resistances of the formed oxide layers give a small potential drop compared to that of the cathode current collector.

Keywords: Molten carbonate fuel cell (MCFC); Corrosion; Reducing environment; Anode current collector

1. Introduction

Molten carbonate fuel cells (MCFC) are fuel cells operating at about 650 °C with molten lithium/potassium carbonate or lithium/sodium carbonate as electrolyte. They are most suitable for stationary applications and in particular their high operation temperature makes it possible to use cheaper materials such as nickel as electrodes instead of more noble metals used in low temperature fuel cells. Furthermore, hydrocarbons and carbon monoxide can directly be utilised as fuels and the waste heat has high quality, leading to an over-all efficiency of at least 80%. Operating at 650 °C in an oxidising and/or reducing environment with a molten salt present for several years generates some material challenges. Corrosion of metallic parts (current collectors and wet-seal material) is one of the life-time limiting factors for MCFC, and research in this area has been on-going for more than 20 years. The metallic parts in MCFC systems often suffer from hot corrosion where the oxide layer is attacked by the molten salt, dissolved and re-precipitated again, causing a porous non-protective oxide layer that do not hinder further attacks on the material. Moreover, the corrosion processes often cause a permanent loss of electrolyte by forming corrosion products containing lithium or potassium. The corrosion can cause over 20% of the total electrolyte loss during operation [1]. Besides causing material damage, corrosion may also affect the efficiency of the system. The oxide layer formed by the corrosion can have a high resistance that results in a decrease in cell potential. This voltage drop has been investigated by various researchers [2–5] for the cathode current collector. For stainless steel 310, the voltage drop of the formed oxide layer can be as much as 80 mV at 1600 A m^{-2} [2], and limits the use of SS 310 as cathode current collector, although it has a lower corrosion rate than SS 316L.

Corrosion of the metallic parts occurs on both the anodic and cathodic side of the cell. A theoretical study of the wet-seal area made by Donado et al. [6] concluded that the driving force on the cathode side is larger under open circuit potential (OCP) than under load, while on the anode side, the driving force is larger under load than under OCP. For the anode side, this was confirmed by experiments [7]. Anode side corrosion is usually regarded as the most severe [8,9], since the corrosion rate is higher at the anode side for many materials [7,10], and the oxidising agent is water dissolved in the melt [10,11].

Nickel, which is thermodynamically stable in anode environment, is too expensive to have as anode current collector material. Instead, cladding a thin nickel layer on cheaper stainless steel (Ni-clad) has been a way to combine the lower price and better mechanical stability of the stainless steel with the

* Corresponding author. Fax: +46 8 10 80 87.
E-mail address: sara.randstrom@ket.kth.se (S. Randström).

0378-7753/$ – see front matter © 2006 Elsevier B.V. All rights reserved.
doi:10.1016/j.jpowsour.2006.04.069

Table 1
Additions in alloys used as anode current collector material

Element	Reference
Aluminium (Al)	[5,11,13,15–17]
Manganese (Mn)	[14]
Cerium (Ce)	[14]
Lanthanum (La)	[14]
Yttrium (Y)	[5,11,15–17]
Molybdenum (Mo)	[14]
Titanium (Ti)	[5,11]

good chemical stability of nickel in anode environment. The endurance of this material is usually considered to be sufficient for the life-time goal for MCFC (40,000 h) if the nickel layer is thick enough, and Ni-clad has been widely used as anode current collector material. However, nickel clad on stainless steel is an expensive material and internal oxidation can occur as shown by Huijsmans et al. [1], resulting in a rapidly destroyed base material. Therefore, a cheaper material is desired, preferably an alloy. The desired alloy should have the following properties:

- good conductivity of both metal and oxide layer, if formed;
- cheap, both in manufacturing and treatment;
- good mechanical properties, i.e. not too soft in order to avoid deformation under pressure but soft enough to be machined easily;
- corrosion products that do not contaminate the electrolyte or precipitate in the electrodes, since corrosion on both anode and cathode current collectors can form corrosion products that dissolve in the melt [12].

The alloys considered are often high nickel and/or high chromium alloys since both nickel and chromium have beneficial effects on corrosion resistance in anode environment [5,13]. Many other elements may be added to the alloy in order to improve the material properties. Table 1 lists some elements which have been investigated in MCFC anode environment. In all cases the base alloy is composed of at least two of the three elements; Fe, Ni and Cr.

Although many researchers have proceeded from using an alloy to a bi-metallic design, some promising results have been published [5,15–17] using an alloy showing good resistance to corrosion in both anode and cathode environment. The alloy is a high nickel, high chromium alloy stabilised by small additions of yttrium and aluminium. The small additions of yttrium and aluminium increase the stability and decrease the corrosion rate [17].

In this study, small-scale molten carbonate fuel cells have been operated with different current collector materials in anode environment. During operation, the resistance of the oxide layer was measured, and after shut down of the cell, the anode current collector and anode were analysed in a scanning electron microscope (SEM) equipped with energy dispersive spectrometer (EDS).

2. Experimental

Circular lab-scale molten carbonate fuel cells with a geometric area of 3 cm^2 were operated at 650 °C unless otherwise stated, in a setup similar to that used in [2]. The experimental setup is shown in Fig. 1. A gold wire, protected by an alumina tube, was inserted in a tube in the middle of the anode current collector and had direct contact with the anode (Probe 2). A stainless steel wire was point-welded in the edge of the anode current collector (Probe 1). This enabled a direct measurement of the oxide layer of the anode current collector and was described in an earlier paper [2].

The electrolyte used in all experiments was eutectic lithium and potassium carbonate ($(Li_{0.62}K_{0.38})_2CO_3$) and was of pro analysi grade (Merck). The anode used was a nickel anode stabilised by chromium. Anode current collector materials were either nickel clad on stainless steel or a high chromium, high nickel alloy, stabilised by yttrium and aluminium (hereafter called Alloy A) or a commercial high temperature alloy with other additives, hereafter called Alloy B.

2.1. Manufacturing of the anode current collector

The anode current collectors were cut from a sheet of the material and 18 gas holes (Ø2.2 mm) were drilled, except in the

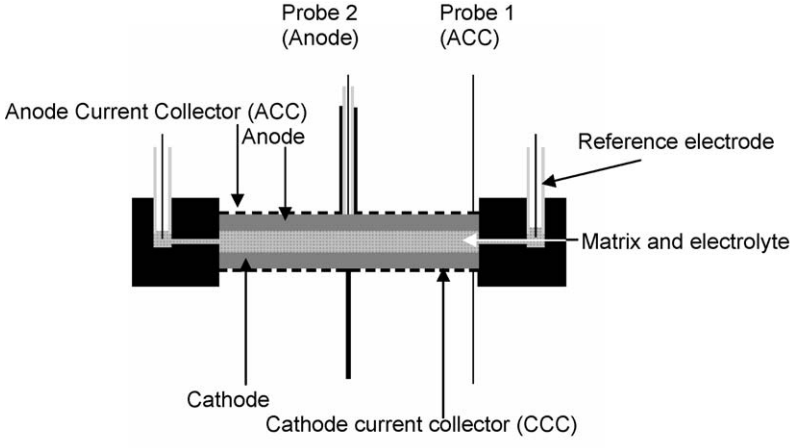

Fig. 1. Principal sketch of the experimental setup for the electrochemical measurements.

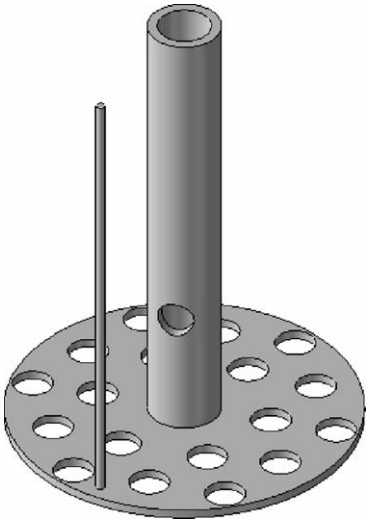

Fig. 2. Design of anode current collector, $Ø_{disc}$ = 19 mm, $Ø_{hole}$ = 2.2 mm.

case of nickel clad on stainless steel, where one of the anode current collector discs was made by laser. The design of the current collectors used can be seen in Fig. 2. The anode current collector disc (Ø19 mm) was then attached to a tube by a rivet and holes were drilled in the tube. These holes ensured that the anode probe encountered the same environment as the anode current collector.

Thereafter, the anode current collectors were polished with SiC abrasive papers (at least #1200), washed with distilled water and acetone and thereafter dried. The Ni-clad anode current collectors were not polished, since the thin layer of nickel could be destroyed.

2.2. Cell heating and electrochemical experiments

During heat-up of the single cell, nitrogen was used. At 580 °C two weights were put on top of the cell with a total weight of 2 kg and the gases were switched to anode and cathode gas. The gas on the anode side consisted of 64% H_2, 20% H_2O and 16% CO_2 and at the cathode side the gas consisted of 14% O_2, 4% H_2O, 29% CO_2 and 53% N_2. The flows were 113 ml min^{-1} (dry gas) at the cathode side and 109 ml min^{-1} (dry gas) at the anode side. During measurements the anode and cathode flows were increased to 186 ml min^{-1} (dry gas) and 150 ml min^{-1} (dry gas), respectively. The cell setup enabled carbonate additions during the experiment and small pieces of carbonate (6–12 mg) were added on top of the anode current collector. The polarisation of the electrodes varies with the fill degree [18] and carbonate was added so that the polarisation was minimised.

All cells were operated under load, usually at 1600 A m^{-2}, except for one of the cells with Ni-clad, which was operated at a lower current density due to a lower performance. The corrosion behaviour can be different under load than at open circuit potential and is usually considered more severe under load [6]. Electrochemical measurements were done with a Solartron 1287 or Solartron 1286 potentiostat. The potential drop between the anode and the anode current collector was measured galvanostatically during the operation time, and the resistance of the oxide layer was given by Ohm's law. The cells were operated for different times, as shown in Table 2.

2.3. Post-test analysis

After the cells were shut down, the package with anode and anode current collector was put in epoxy, cut and polished with ethanol. These cross-sections were cut so that a part of a hole could always be analysed. Post-test analyses of the cross-sections were made with a SEM, JEOL JSM-840, equipped with EDS.

3. Results and discussion

3.1. Electrochemical measurements

For all materials tested the electrochemical resistance of the oxide layer was lower than on the cathode side [2–4]. For nickel clad on stainless steel it was not possible to detect any electrical resistance between the anode and the anode current collector. Since nickel is thermodynamically stable in anode atmosphere, this material should not form any oxide layer. This is well in agreement with statements found in literature [19]. For Alloy A, the results were not reproducible, the resistance varied between the measurements and also the shapes of the two curves were different as seen in Fig. 3. In cell 4, the curve had a logarithmic shape while in cell 5, the resistance was almost constant for 1000 h and then increased rapidly. For Alloy B, the resistance remained at a low and constant level during the 2000 h operated. The resistances were small and resulted in very small iR drops, e.g. 1.5 μΩ m^2 corresponded to an iR drop of 2.4 mV when operating at 1600 A m^{-2}.

Table 2
Operation times and materials used in the different cells operated

Cell no.	Anode current collector material	Comment	Operation time (h)
1	Ni-clad on stainless steel (drill)	Low cell performance	368
2	Ni-clad on stainless steel (drill)	–	820
3	Ni-clad on stainless steel (laser)	*T*: 670 °C	724
4	Alloy A	–	654
5	Alloy A	Carbon deposition found	2064
6	Alloy B	–	2000

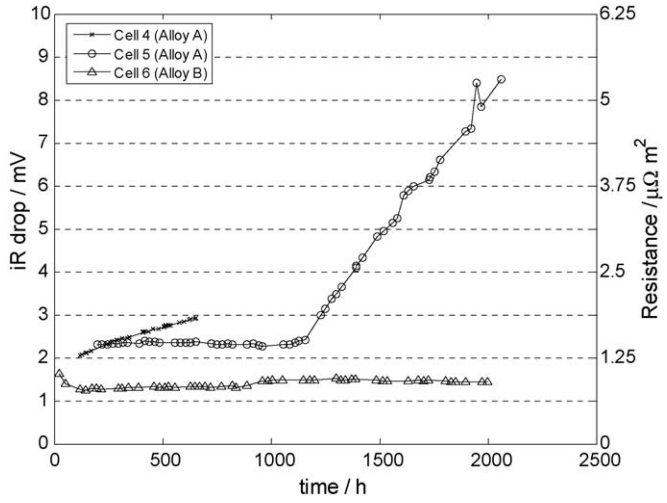

Fig. 3. Electrical resistance and iR drop at 1600 A m^{-2} between the anode and anode current collector of the operated cells.

3.2. Post-test analysis

3.2.1. Ni-clad on stainless steel

SEM and EDS analysis showed, as expected, that no oxide layer was present. Some iron and chromium had diffused into the nickel layer, this phenomenon was also observed by Yuh et al. [19]. At the edge of the holes, a distinct difference between the cell with drilled holes and the one with laser made holes could be seen (Fig. 4). When drilling, the mechanical stress caused a detachment of the nickel layer and a crevice was formed during operation, seen as a darker triangle in the left part of Fig. 4. The crevice expanded with time. EDS analysis of the compounds found in the crevice showed that chromium and oxygen was present in the ratio 1:2 (at.%). Vossen et al. [20] concluded that $LiCrO_2$ is the stable chromium oxide in anode environment. The compound found was therefore probably $LiCrO_2$. However, lithium was too light to be detected by the instrument. Iron was also found at some points in the crevice and there were brighter areas enriched in nickel. When making the anode current collectors with laser, a small cap was formed surrounding the chromium oxides formed at the wall of the hole, as seen in the right part of Fig. 4.

In the clad nickel layer small defects were found after operation as seen in the right part of Fig. 5. These had evolved during operation since SEM investigation of an un-operated material did not show these voids (Fig. 5, left).

3.2.2. Alloy A

Fig. 6 shows SEM micrographs of the current collectors near a drilled gas hole from cell 4 (left) and cell 5 (right), respectively, both operated with Alloy A as anode current collector material. EDS analysis of the current collector from cell 4 (Fig. 6, left), operated for a shorter time (654 h), showed a chromium rich oxide with small nickel islands, seen as light stripes in the darker oxide layer. The oxide layer had fallen off and new chromium oxides were formed at the base material. The base material was unaffected, except from a region near the oxide layer, where it was chromium depleted. The chromium oxide was probably $LiCrO_2$, the ratio between chromium and oxygen was about 1:2

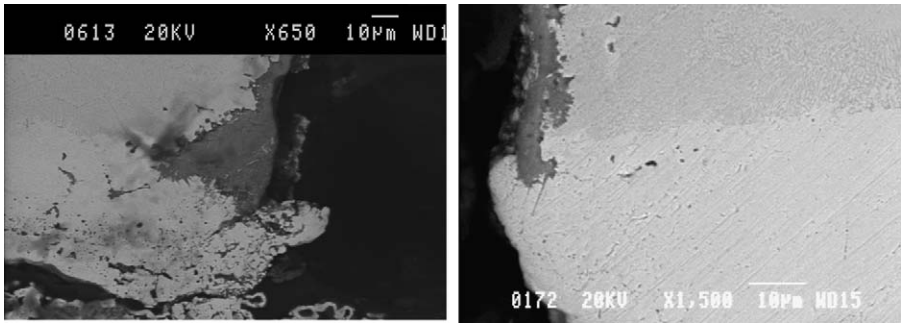

Fig. 4. Comparison between nickel clad on stainless steel, with holes made by drill (left) and laser (right) after 368 and 724 h, respectively.

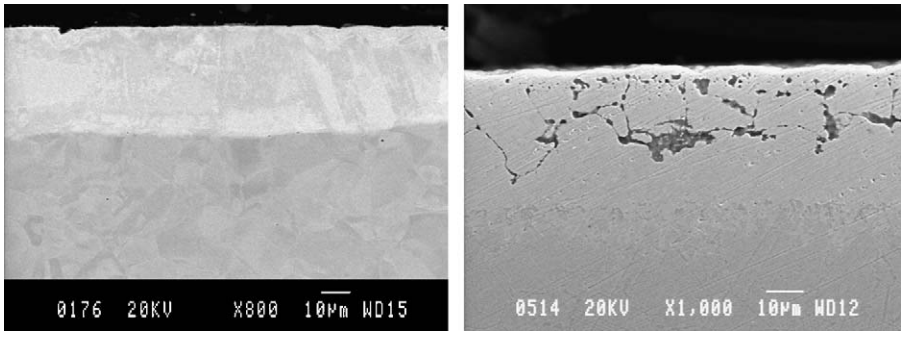

Fig. 5. SEM micrograph of nickel layer before (left) and after 820 h (right) of operation.

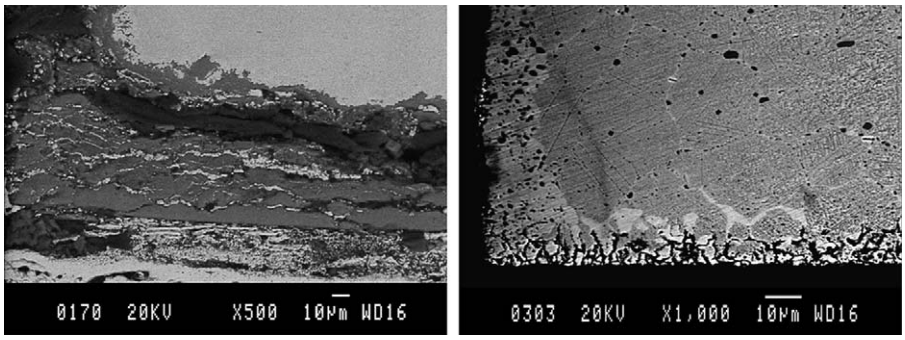

Fig. 6. SEM micrograph of Alloy A after 654 h (left) and 2064 h (right).

Table 3
Compositions at some points close to the anode for an anode current collector made of alloy A

Point	Fe	Cr	Ni	Al	Y	O
1	19	10	32	10	–	29
2	26	10	47	4	–	12
3	23	18	42	5	–	12
4	24	17	45	2	–	12
5	16	52	28	2	1	–

All numbers given in at.%. The positions of the points can be seen in Fig. 7.

and as discussed earlier, $LiCrO_2$ is assumed to be the oxide formed in anode environment.

SEM and EDS analyses from cell 5 (Fig. 6, right) operated for 2064 h, showed a different structure of the current collector than that of the cell operated for 654 h. The part of the anode current collector closest to the anode (lower part in the right of Fig. 6) had a porous structure in which the composition varied. In Table 3, the composition for different points are given, with points 1 and 2 close to the anode, and points 3–5 a little bit higher up, the positions of the points are shown in Fig. 7. At points 1 and 2, found close to the anode, the material was chromium depleted and enriched in aluminium. Also, at points 3 and 4, found further from the anode, the material was chromium depleted, while at point 5 it was actually enriched in chromium.

Besides the most affected area closest to the anode, the material in the middle of the current collector was also affected and areas enriched in nickel (around 50 at.%) were found, in the right part of Fig. 6 seen as lighter areas. The grain boundaries were visible, and substantially enriched in chromium, but no carbon could be detected by EDS analysis. In the anodic atmosphere there is a risk of carburisation [12] and formation of carbides, since the carbon activity is high, especially beneath an oxide scale. The carburisation can cause brittleness in the material.

When disassembling cell 5, it could be seen that carbon had deposited 5 cm above the current collector. This phenomenon could not be seen when disassembling the other cells. If this is the reason to the different corrosion behaviour of the two anode current collectors made of Alloy A is not known for sure, but carbon deposition indicates that the water content has not been sufficiently high. If the water content has been low, this has affected the oxygen pressure and eventually this could have influenced the oxide formation. Another possible explanation is

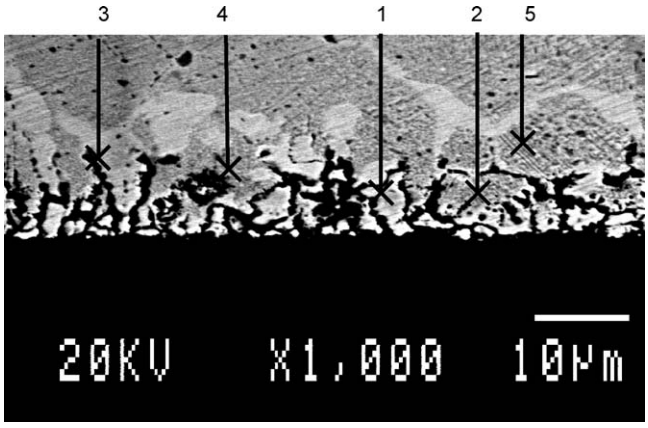

Fig. 7. Detailed view of Fig. 6, right. The numbers refer to Table 3.

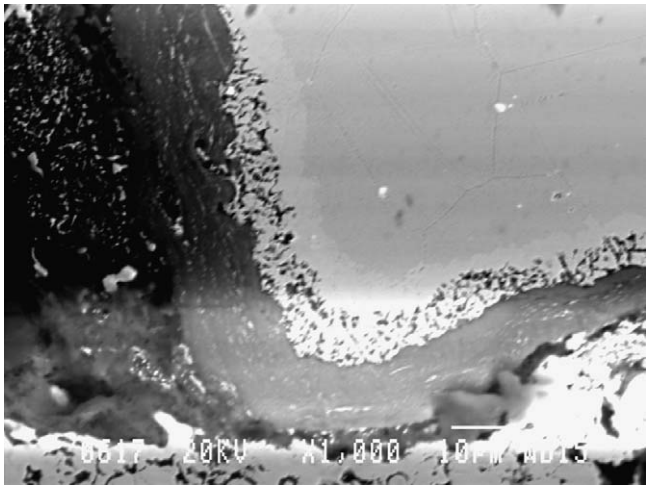

Fig. 8. SEM micrograph of Alloy B after 2000 h of operation.

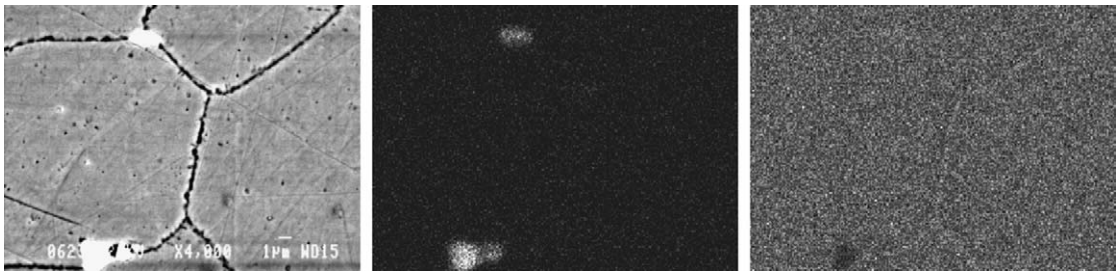

Fig. 9. SEM micrograph of grain boundary of Alloy B and mapping of additive (middle) and Cr (right).

the absence of a dense and well adherent oxide layer in cell 4. The detachment of the oxide layer could go on to a point where the material is chromium depleted, but since $LiCrO_2$ does not seem to be soluble in molten carbonate [12], this compound should have been present when analysing the anode current collector from cell 5 in SEM/EDS.

3.2.3. Alloy B

Except the base of iron, chromium and nickel, Alloy B contains additions of elements which are known for their ability to form alloys with a resistance to carburisation and hot corrosion. SEM analysis of the material after 2000 h of operation (Fig. 8), showed that a dense and well adherent oxide layer had formed consisting of chromium oxides. In addition, the ratio between chromium and oxygen was 1:2 and the chromium oxide formed was therefore probably $LiCrO_2$. Small bright stripes were present in the oxide layer, and the base material closest to the oxide layer was depleted in chromium. Looking closer, the grain boundaries were clearly visible as seen in the left part of Fig. 9. One of the additives, known for its ability to prevent chromium carbide formation, was present in the grain boundaries, not evenly spread, but gathered in spots as shown in Fig. 9, middle. The grain boundaries were instead slightly enriched in chromium (right part of Fig. 9), which leads to the conclusion that the additive was not preventing chromium carbide formation at the grain boundaries.

4. Conclusions

The electrical resistance and behaviour of three different anode current collector materials have been tested in a small scale molten carbonate fuel cell. The difference in electrical resistance between the tested materials was small. For all materials, the voltage drop of the oxide layers found was not larger than a few millivolts. Instead, the problems with the anode current collector materials tested were that the oxide layer formed was not protective and that carburisation occurred.

Nickel clad on stainless steel did not form any oxide layer and hence the contact resistance was zero. Small defects could be seen in the nickel layer after operation, and the nickel layer detached if mechanically treated.

The high nickel, high chromium alloy stabilised by yttrium and aluminium is not a good candidate material to use as anode current collector material. After 654 h an oxide layer was formed, but the adherence of the oxide layer was poor. After 2000 h, the material was destroyed, the layer closest to the anode had voids and a homogeneous oxide layer was absent.

However, the commercial alloy tested could be a possible candidate to use as anode current collector. The oxide layer was dense and well adherent, although some chromium enrichment was seen in the grain boundaries indicating that chromium carbide was formed, which could be a problem when operating for longer times.

Acknowledgements

This work is a part of the IRMATECH project. The European Commission is gratefully acknowledged for the financial support.

References

[1] J.P.P. Huijsmans, G.J. Kraaij, R.C. Makkus, G. Rietveld, E.F. Sitters, H.Th.J. Reijers, J. Power Sources 86 (2000) 117–121.
[2] B. Bergman, C. Lagergren, G. Lindbergh, S. Schwartz, B. Zhu, J. Electrochem. Soc. 148 (1) (2001) A38–A43.
[3] A.C. Schoeler, T.D. Kaun, M. Krumpelt, Mater. Corros. 51 (2000) 797–807.
[4] A.C. Schoeler, T.D. Kaun, I. Bloom, M. Lanagan, M. Krumpelt, J. Electrochem. Soc. 147 (3) (2000) 916–921.
[5] P. Biedenkopf, M.M. Bischoff, T. Wochner, Mater. Corros. 51 (2000) 287–302.
[6] R.A. Donado, L.G. Marianowski, H.C. Maru, J.R. Selman, J. Electrochem. Soc. 131 (11) (1984) 2535–2540.
[7] R.A. Donado, L.G. Marianowski, H.C. Maru, J.R. Selman, J. Electrochem. Soc. 131 (11) (1984) 2541–2544.
[8] C. Yuh, J. Power Sources 56 (1995) 1–95.
[9] W. Vielstich, H.A. Gasteiger, A. Lamm (Eds.), Handbook of Fuel Cells—Fundamentals, Technology and Applications, vol. 4: Fuel Cell Technology and Applications, John Wiley & Sons, Chichester, 2003.
[10] J.R. Selman, in: L.J.M.J. Blomen, M.N. Mugerwa (Eds.), Fuel Cell Systems, Plenum Press, New York, 1993, pp. 345–463.
[11] G. Lindbergh, B. Zhu, Electrochim. Acta 46 (2001) 1131–1140.
[12] P. Singh, in: J.R. Selman, T.D. Claar (Eds.), Molten Carbonate Fuel Cell Technology, PV 84-13, The Electrochem. Soc., Inc., Pennington, NJ, 1984, pp. 124–139.
[13] J.P.T. Vossen, L. Plomp, J.H.W. de Wit, G. Rietveld, J. Electrochem. Soc. 142 (10) (1995) 3327–3335.
[14] Energy Research Corporation, Final Rep. US DOE under Contract No. DE-AC21-84MC21186.
[15] T. Shimada, N. Ariga, J. Sakai, K. Masamura, Trans. Mater. Res. Soc. Jpn. 18A (1994) 569–571.
[16] T. Shimada, Y. Kuriki, N. Yamanouchi, M. Tamura, 1990 Fuel Cell Seminar, Tucson, AZ, USA, November 25–28, 1990, pp. 171–174.

[17] T. Yoshii, K. Hishino, N. Ariga, M. Yamamoto, Y. Horii, 1994 Fuel Cell Seminar, San Diego, CA, USA, November–December, 1994, pp. 140–143.
[18] C. Lagergren, A. Lundblad, B. Bergman, J. Electrochem. Soc. 141 (11) (1994) 2959–2966.
[19] C. Yuh, R. Johnsen, M. Faroque, H. Maru, in: D. Shores, H. Maru, I. Uchida, J.R. Selman (Eds.), Carbonate Fuel Cell Technology, PV 93-3, The Electrochem. Soc., Inc., Pennington, NJ, 1993, pp. 158–170.
[20] J.P.T. Vossen, R.C. Makkus, J.H.W. de Wit, J. Electrochem. Soc. 143 (1) (1996) 66–73.